

# Neutrino factory near detector simulation

Yordan Karadzhov, Roumen Tsenov  
Department of Atomic Physics,  
St. Kliment Ohridski University of Sofia,  
Sofia, Bulgaria

October 23, 2009

## 1 Introduction

The aim of the Near detector of the Neutrino factory is to measure precisely the absolute neutrino flux, the neutrino cross sections and to estimate the background to the far detector. Results presented here continue our efforts on Near detector simulation performed for the ISS [1]

## 2 Muon decay matrix element

The probability for having a neutrino with a given energy and polar angle in the rest system of the muon is given by the following matrix elements :

$$\text{for } \nu_\mu : \quad \frac{d^2 N}{dx d\Omega} \sim ((3 - 2x) + \cos\theta P_\mu(1 - 2x))x^2, \quad (1)$$

$$\text{for } \bar{\nu}_e : \quad \frac{d^2 N}{dx d\Omega} \sim ((1 - x) + \cos\theta P_\mu(1 - x))x^2, \quad (2)$$

where  $x = 2E_\nu/m_\mu$  ,  $P_\mu$  is the polarization of the muon and  $\theta$  is the angle between the polarization vector and the neutrino direction [2].

## 3 Quasielastic scattering off electrons in the near detector

The quasielastic scattering off electrons is suitable for measurement of the neutrino flux, because its absolute cross-section can be calculated theoret-

ically with enough confidence. The two processes of interest for neutrinos from  $\mu^-$  decays are:

$$\nu_\mu + e^- \rightarrow \nu_e + \mu^- \quad (3)$$

and

$$\bar{\nu}_e + e^- \rightarrow \bar{\nu}_\mu + \mu^- \quad (4)$$

For the process (3) the cross section is isotropic in the c.m. system and is given by :

$$\sigma = \frac{G_F^2 (s - m_\mu^2)^2}{\pi s} \quad (5)$$

For the process (4) the differential cross section in the c.m. system is given by :

$$\begin{aligned} \frac{d\sigma}{d\cos\theta} &= \frac{G_F^2 (s - m_\mu^2)^2}{\pi s} \times \\ &\left(1 + \frac{s - m_\mu^2}{s + m_\mu^2} \cos\theta\right) \left(1 + \frac{s - m_e^2}{s + m_e^2} \cos\theta\right) \end{aligned} \quad (6)$$

and the total cross section is:

$$\sigma = \frac{G_F^2 (s - m_\mu^2)^2}{\pi s^2} \left(E_e E_\mu + \frac{1}{3} E_{\nu 1} E_{\nu 2}\right), \quad (7)$$

where  $E_{\nu 1}$  and  $E_{\nu 2}$  are the energies of the neutrinos. They depend, in turn, only on  $s$ .

For neutrinos coming from decays of unpolarized muons the cross-section of (4) is an order of magnitude smaller than that of (3).

## 4 Simulation of the neutrino flux in the Near detector and its measurement

The input parameters of the simulation of the beam are:

- length of the straight section of the muon storage ring: 600 m;
- muon beam energy: 25 GeV;

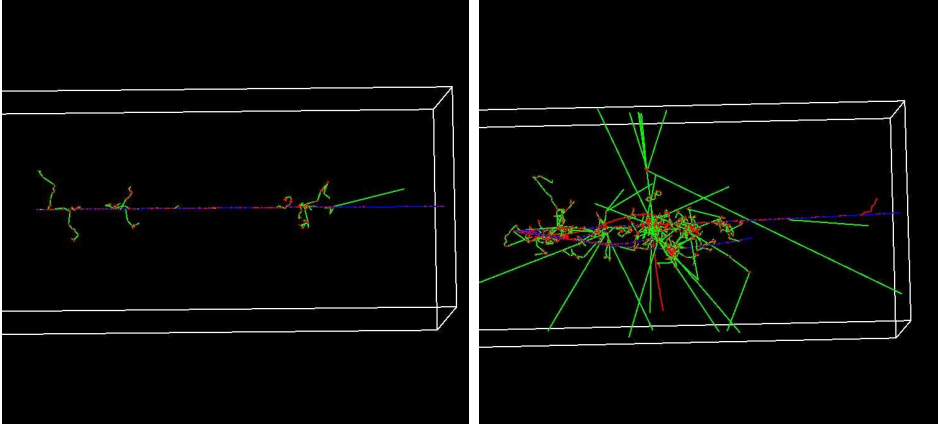


Figure 1: Visualization of a leptonic event (left) and  $\nu N$  CC event (right) from a GEANT4 simulation.

- muon energy distribution: Gaussian ( $\sigma = 80 \text{ MeV}$ );
- muon angular distribution: Gaussian ( $\sigma = 0.5 \text{ mrad}$ ).

Results below are based on  $6.24 \times 10^{16}$  simulated muon decays (approx. 1 hour of work of Neutrino factory), while event rates on some of the plots are scaled to the nominal number of  $5 \times 10^{20}$  muon decays per year.

If we want to measure the neutrino flux by using the quasielastic scattering off electrons (3, 4) (for earlier measurements of these processes see, e.g. [3, 4]), the detector has to be able to distinguish between the two types of events shown in Fig. 1.

The neutrino event generator GENIE [5, 6] has been used to simulate the interactions of the neutrinos with a cylindrical detector, 5 m long and with radius of 2 m, made of polystyrene ( $\rho = 1.032 \text{ g/cm}^3$ ). The nominal detector position has been chosen at 100 m after the decay ring straight section. Fig. 2 demonstrates the dependence of the event rate on the distance from the straight section end and Fig. 3 represents the variation with the distance from the beam axis.

Kinematical distributions of the events are demonstrated on Figs. 4, 5, 6, 7.

It is considered that the detector will be able to measure the angle between the beam axis and the direction of the outgoing muon  $\theta_\mu$ , the momentum of the outgoing muon  $p$ , thus its energy  $E_\mu$  and transverse momentum  $p_\perp$ , and the total recoil (hadronic) energy  $E_{had}$  with certain resolution.

Several scenarios for the resolutions have been adopted:

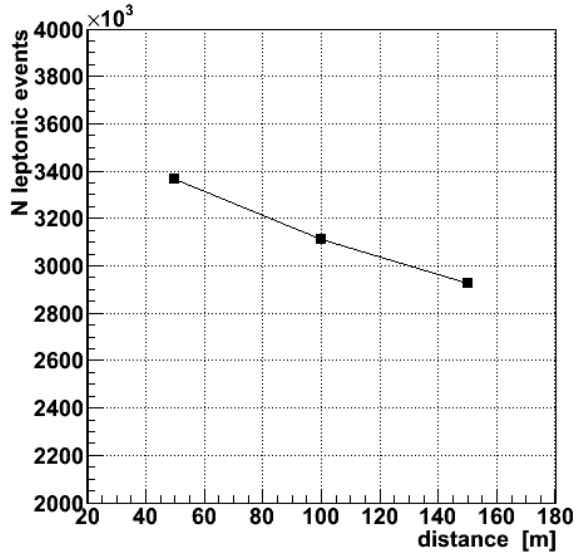


Figure 2: Number of pure leptonic neutrino interactions from the process (3) in the near detector at three different distances from the straight section end. The scale on the ordinate axis is normalized to  $5 \times 10^{20}$  muon decays.

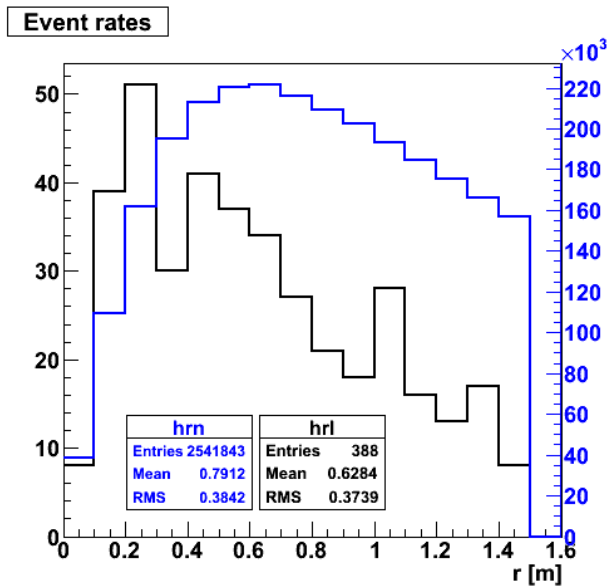


Figure 3: The event rates from inclusive  $\nu N$  scattering (blue histogram, right scale) and leptonic scattering (3) (black histogram, left scale) at 100 m after the end of the straight section versus the distance from the beam axis.

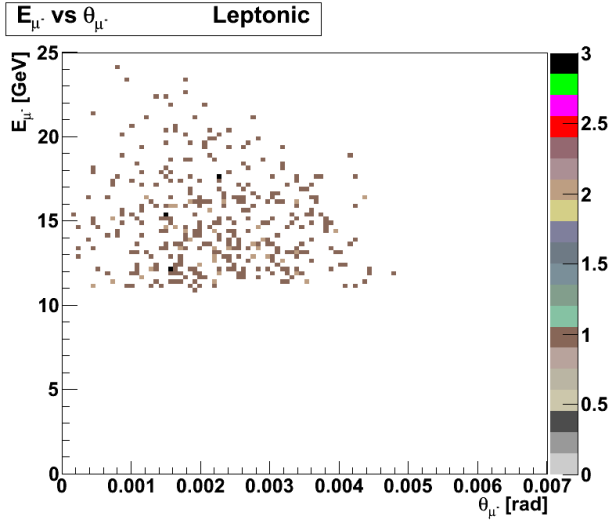


Figure 4: Energy of the scattered muon versus its scattering angle for the process (3). The shape of the distribution is determined entirely from the muon decay kinematics and muon beam spread.

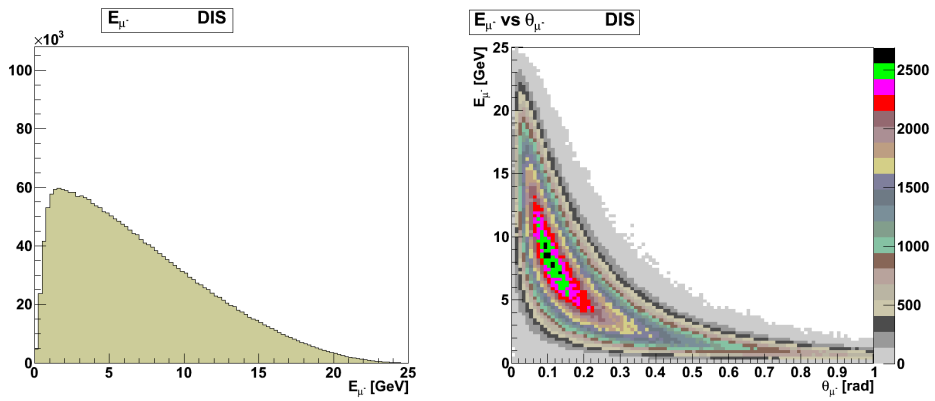


Figure 5: Energy of the scattered muon versus its scattering angle for inclusive  $\nu N$  process.

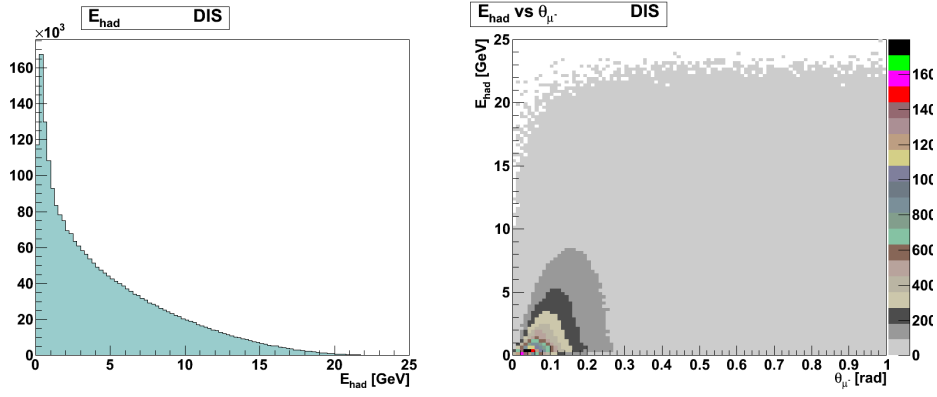


Figure 6: Recoil (hadron) energy versus muon scattering angle for inclusive  $\nu N$  process.

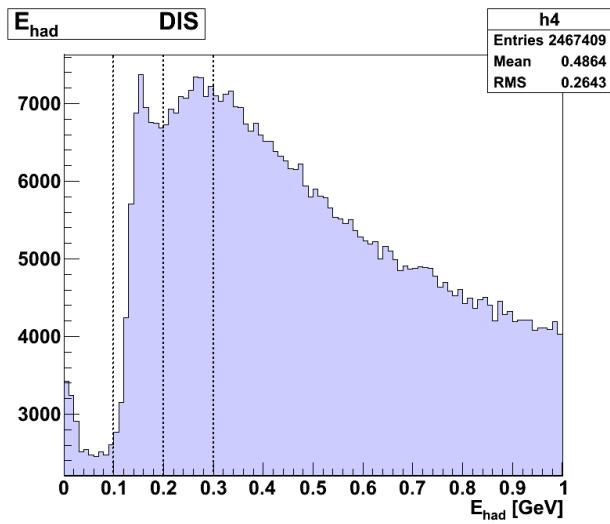


Figure 7: Distribution of the recoil (hadronic) energy below 1 GeV for inclusive  $\nu N$  process. Cuts at 100, 200 and 300 MeV are shown with vertical lines.

- poor resolutions:

$$\sigma(\theta) = 1.0 \text{ mrad}; \quad \frac{\sigma(E_\mu)}{E_\mu} = 10\% : \quad \frac{\sigma(E_{had})}{E_{had}} = 10\%; \quad (8)$$

- medium resolutions:

$$\sigma(\theta) = 0.5 \text{ mrad}; \quad \frac{\sigma(E_\mu)}{E_\mu} = 5\%; \quad \frac{\sigma(E_{had})}{E_{had}} = 5\%; \quad (9)$$

- best resolutions:

$$\sigma(\theta) = 0.1 \text{ mrad}; \quad \frac{\sigma(E_\mu)}{E_\perp} = 1\%; \quad \frac{\sigma(E_{had})}{E_{had}} = 1\%. \quad (10)$$

Different variables for suppression of the background from inclusive  $\nu N$  CC reactions have been examined:

- muon scattering angle;
- transverse momentum;
- $E_\mu * \theta_\mu^2$ ;
- recoil (hadronic) energy.

Spectra of the events over smeared  $\theta_\mu$  and  $E_\mu * \theta_\mu^2$  for the *poor* and *best* resolutions scenario and for cuts on the recoil energy depicted on Fig. 7 are shown on Figs. 9, 10.

It is seen that by imposing suitable cut on the recoil energy and subtracting the fitted inclusive background under the peak it is possible to determine statistically the number of events due to pure leptonic scattering with a precision of a few percent. Both variables  $\theta_\mu$  and  $E_\mu * \theta_\mu^2$  may be used for this task. For a decisive choice more detailed simulation of the background with  $\theta_\mu \rightarrow 0$  is needed. It was shown earlier (see Y. Karadzov's contribution to NUFACT09) that  $p_\perp$  is less efficient than  $\theta_\mu$  for signal extraction.

In Fig. 8 we present a table with our numerical results.

## 5 Conclusions

The quasielastic scattering off electrons can be used to measure the neutrino flux coming from the Neutrino factory storage ring.

$\theta$	cut value	Purity [%]	Signal	All evts	Bkgr	Bkgr evts	
	[rad]		evts	below	evts	deduced	
				the cut		from the fit	
v1	$E_{\text{had}} < 100\text{MeV}$	0.0055	66	388	582	205	262 +- 37
v2	$E_{\text{had}} < 100\text{MeV}$	0.0055	72	388	536	152	210 +- 34
v3	$E_{\text{had}} < 100\text{MeV}$	0.0055	73	388	528	140	175 +- 30
v1	$E_{\text{had}} < 200\text{MeV}$	0.0060	31	388	1216	836	830 +- 100
v2	$E_{\text{had}} < 200\text{MeV}$	0.0050	42	388	913	533	641 +- 72
v3	$E_{\text{had}} < 200\text{MeV}$	0.0050	42	388	922	538	544 +- 63
v1	$E_{\text{had}} < 300\text{MeV}$	0.0050	30	388	1261	898	990 +- 90
v2	$E_{\text{had}} < 300\text{MeV}$	0.0045	36	388	1058	693	656 +- 62
v3	$E_{\text{had}} < 300\text{MeV}$	0.0045	37	388	1031	658	639 +- 62
<b><math>\theta^2 * E_{\mu}</math> [rad<sup>2</sup>*GeV]</b>							
v1	$E_{\text{had}} < 100\text{MeV}$	0.42	63	388	608	237	273 +- 13
v2	$E_{\text{had}} < 100\text{MeV}$	0.42	68	388	565	179	229 +- 12
v3	$E_{\text{had}} < 100\text{MeV}$	0.42	70	388	551	163	216 +- 11
v1	$E_{\text{had}} < 200\text{MeV}$	0.36	37	388	1034	669	793 +- 19
v2	$E_{\text{had}} < 200\text{MeV}$	0.36	37	388	1030	652	800 +- 19
v3	$E_{\text{had}} < 200\text{MeV}$	0.30	44	388	870	493	677 +- 15
v1	$E_{\text{had}} < 300\text{MeV}$	0.36	27	388	1436	1071	1286 +- 24
v2	$E_{\text{had}} < 300\text{MeV}$	0.36	27	388	1436	1058	1267 +- 24
v3	$E_{\text{had}} < 300\text{MeV}$	0.36	27	388	1394	1011	1266 +- 23

Figure 8: Numerical results of the procedure for background subtraction. *Purity* is defined as the true number of leptonic events divided by the total number of events below the cut value of the respective variable. *v1* stands for *poor* resolutions, *v2* - for *medium* and *v3* - for the *best* one.

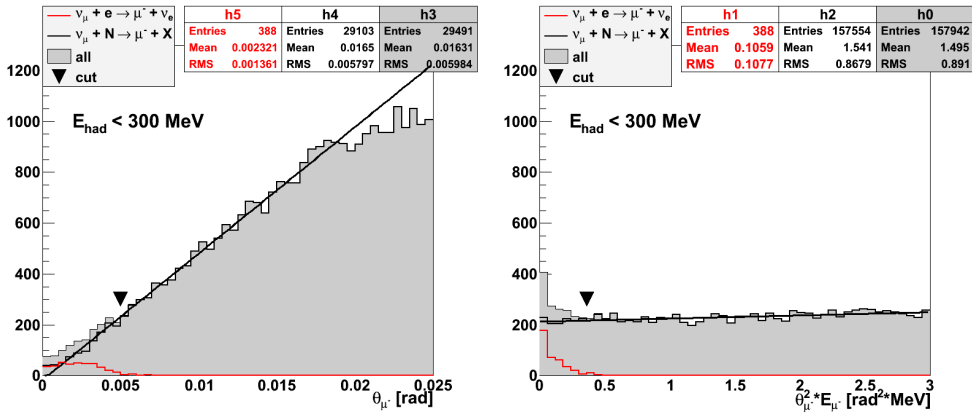


Figure 9: “Measured” distributions of the outgoing muons in the so called *poor* scenario (see the text). The leptonic events are in red, the hadronic events are in black and the total spectrum is filled with gray. The cut value is denoted by black inverted triangle.



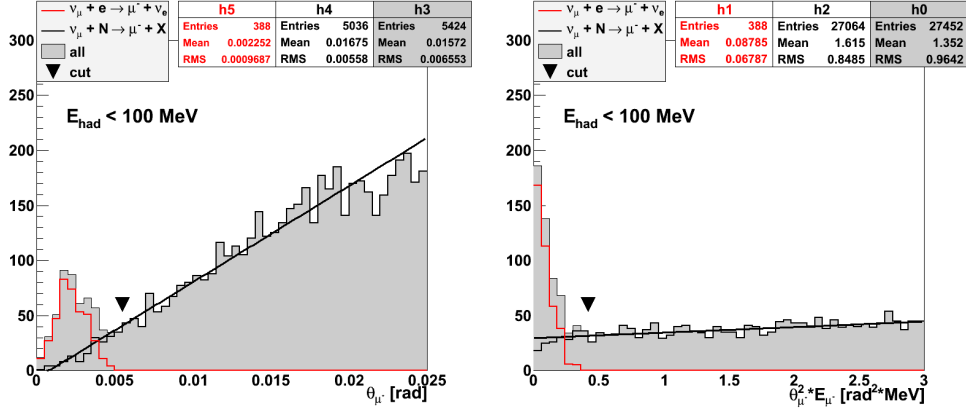


Figure 10: “Measured” distributions of the outgoing muons in the so called *best* scenario (see the text). The leptonic events are in red, the hadronic events are in black and the total spectrum is filled with gray. The cut value is denoted by black inverted triangle.

For chosen resolutions on  $\theta_\mu$ ,  $E_\mu$  and  $E_{had}$ , the angle  $\theta_\mu$  and the composite variable  $E_\mu * \theta_\mu^2$  have similar discriminating power. The last one seems to have flatter distribution when  $\theta_\mu \rightarrow 0$ .

The confidence on the measurement of  $E_{had}$  down to few tens of *MeV* is critical for the selection.

Our plans for the next year include:

- specification of detector design and size;
- full GEANT4 simulation to obtain “true” values of the measurables;
- implementation of some reconstruction and obtaining of “measured” values;
- definition of a procedure for flux determination based on statistical subtraction of the inclusive background and estimation of expected uncertainties.

## References

- [1] T. Abe et al., Detectors and flux instrumentation for future neutrino facilities, JINST 4 T05001, 2009.
- [2] D. Bardin and V. Dokuchaeva, Nucl. Phys. B287(1987)839.

- [3] P. Vilain et al, Phys. Lett. B 364 (1995) 121.
- [4] S. R. Mishra et al., Phys. Lett. B 252 (1990) 170.
- [5] GENIE web site <http://www.genie-mc.org>.
- [6] C. Andreopoulos et al., The GENIE Neutrino Monte Carlo Generator, arXiv:0905.2517v1.